UCLA
UCLA Previously Published Works

Title
Progression of Geographic Atrophy in Age-related Macular Degeneration AREDS2 Report Number 16

Permalink
https://escholarship.org/uc/item/63p3r3td

Journal
Ophthalmology, 125(12)

ISSN
0161-6420

Authors
Keenan, Tiarnan D
Agrón, Elvira
Domalpally, Amitha
et al.

Publication Date
2018-12-01

DOI
10.1016/j.ophtha.2018.05.028

Peer reviewed

Progresssion of geographic atrophy in age-related macular degeneration: AREDS2 Report number 16

Tiarnan D Keenan, BM, BCh, PhD[1], **Elvira Agrón, MA**[1], **Amitha Domalpally, MD, PhD**[2], **Traci E Clemons, PhD**[3], **Freekje van Asten, MD, PhD**[4], **Wai Wong, MD, PhD**[5], **Ronald G Danis, MD**[2], **SriniVas Sadda, MD**[6], **Philip J Rosenfeld, MD, PhD**[7], **Michael L Klein, MD**[8,9], **Rinki Ratnapriya, PhD**[4], **Anand Swaroop, PhD**[4], **Frederick L Ferris III, MD**[1], **Emily Y Chew, MD**[1], and **for the AREDS2 Research Group**[10]

[1]Division of Epidemiology and Clinical Applications, National Eye Institute, National Institutes of Health, Bethesda, MD, USA

[2]Fundus Photographic Reading Center, The University of Wisconsin, Madison, WI, USA

[3]The Emmes Corporation, Rockville, MD, USA

[4]Neurobiology-Neurodegeneration & Repair Laboratory, National Eye Institute, National Institutes of Health, Bethesda, MD, USA

[5]Unit on Microglia, National Eye Institute, National Institutes of Health, Bethesda, MD, USA

[6]Doheny Eye Institute, Los Angeles, CA, USA

[7]Bascom Palmer Eye Institute, University of Miami Miller School of Medicine, Miami, FL

[8]Casey Eye Institute, Portland, OR, USA

[9]Devers Eye Clinic, Portland, OR, USA

Abstract

Corresponding Author: Emily Y. Chew, MD, NIH, Building 10.CRC, Room 3-2531, 10 Center Dr, MSC 1204, Bethesda, MD 20892-1204, Telephone: 301 496 6583, Fax: 301 496 7295, echew@nei.nih.gov.
[10]Appendix for the listing of all the members of the AREDS2 Research Group

Purpose—To analyze the prevalence, incidence and clinical characteristics of eyes with geographic atrophy (GA) in age-related macular degeneration (AMD), including clinical and genetic factors affecting enlargement.

Design—Prospective cohort study within a controlled clinical trial

Participants—Age-Related Eye Disease Study 2 (AREDS2) participants, aged 50–85 years.

Methods—Baseline and annual stereoscopic color fundus photographs were evaluated for GA presence and area. Analyses included: GA prevalence and incidence rates, Kaplan-Meier rates, mixed-model regression and multivariable analysis of square root of GA area adjusted for covariates including clinical/imagin characteristics and genotype.

Main outcome measures—(i) Presence or development of GA; (ii) change in square root of GA area over time.

Results—At baseline, 517 (6.2%) eyes of 411 (9.8%) participants had pre-existing GA (without neovascular AMD), with the following characteristics: 33% central, 67% non-central and configuration (36% small, 26% solid/unifocal, 24% multifocal, 9% horseshoe/ring and 6% indeterminate). Of the remaining 6530 eyes at risk, 1099 (17.3%) eyes of 883 participants developed incident GA without prior neovascular disease during mean follow-up of 4.4 years. The Kaplan-Meier rate of incident GA was 19% of eyes at 5 years. In eyes with incident GA, 4-year risk of subsequent neovascular AMD was 29%. In eyes with incident non-central GA, 4-year risk of central involvement was 57%. GA enlargement rate (following square root transformation) was similar in eyes with pre-existing GA (0.29mm/year, 95%CI 0.27–0.30) and incident GA (0.28, 0.27–0.30). In the combined group, GA enlargement was significantly faster with non-centrality, multifocality, intermediate baseline size and bilateral GA (p<0.0001 for interaction in each case) but not with AREDS2 treatment assignment (p=0.33) or smoking status (p=0.05). Enlargement was significantly faster with *ARMS2* risk (p<0.0001), *C3* non-risk (p=0.0002) and *APOE* non-risk (p=0.001) genotypes.

Conclusions—Analyses of AREDS2 data on natural history of GA provide representative data on GA evolution and enlargement. GA enlargement, which was influenced by lesion features, was relentless, resulting in rapid central vision loss. The genetic variants associated with faster enlargement were partially distinct from those associated with risk of incident GA. These findings are relevant to further investigations of GA pathogenesis and clinical trial planning.

Introduction

In age-related macular degeneration (AMD), geographic atrophy (GA) is the defining lesion of the atrophic form of late disease. The term was introduced by Gass in 1973 to refer to one or more circumscribed areas of atrophy in the macula that may gradually enlarge and coalesce (1). The atrophy is called geographic as confluent loss of the retinal pigment epithelium (RPE) usually occurs with a sharply demarcated border between depigmented and apparently normal retina (2). Atrophy of the RPE is typically accompanied by atrophy of adjacent photoreceptors and choriocapillaris (3). A common clinical definition for GA in AMD from the Age-Related Eye Disease Study (AREDS) is a sharply demarcated, usually circular zone of partial or complete depigmentation of the RPE, typically with exposure of underlying large choroidal blood vessels, in the absence of neovascular changes in the same

eye (4). The minimum size requirement in AREDS was grading circle I_1 (1/8 disc diameter) and in AREDS2 was grading circle I_2 (1/4 disc diameter), while different studies have specified other size requirements (2, 5).

GA usually begins in the parafoveal region (non-central GA) and takes a variable period of several years to involve the central fovea (central GA) (6). However, a minority of cases exhibit central involvement at first appearance. Areas affected by atrophy are associated with dense scotomata. For this reason, central GA is normally accompanied by very poor visual acuity. Even in individuals where GA is non-central, reduced visual function usually leads to substantial difficulties with reading and facial recognition (7).

GA in AMD is thought to affect over 8 million people worldwide (8). It represents an important clinical and research priority, as no treatments are routinely available in clinical practice to treat GA, prevent its occurrence or decrease its enlargement rate. However, several potential strategies to slow down the enlargement rate of GA are currently under investigation, including those based around inhibition of the complement system (9–11). In these and previous clinical trials, change in GA area over time has been used as the primary outcome measure, with approval of this measure by the FDA as a clinically important endpoint (12–16). For these reasons, natural history data regarding the development and progression of GA may be useful. In addition, information on clinical and genetic factors that influence GA enlargement may provide insights into pathogenesis and may aid recruitment and stratification of patients into clinical trials. For example, some controversy has surrounded the potential role of *CFI* genotype in influencing GA enlargement and response to intravitreal lampalizumab (anti-complement factor D) therapy (17, 18).

The Age-Related Eye Disease Study 2 (AREDS2) was a multicenter phase III randomized controlled clinical trial designed to assess the effects of nutritional supplements on the course of AMD in people at moderate to high risk of progression to late AMD (19). The primary outcome of this clinical trial was development of late AMD, defined as central GA or neovascular AMD. The purpose of this current report was to examine the prevalence, incidence, clinical characteristics and enlargement rate of GA in the AREDS2, in addition to analyzing the influence of clinical characteristics and AMD genotype on enlargement of GA.

Methods

Study population

The study design for AREDS2 has been described previously (19). In short, 4203 participants aged 50 to 85 years were recruited between 2006 and 2008 at 82 retinal specialty clinics in the United States. Inclusion criteria at enrollment were the presence of either bilateral large drusen or late AMD in one eye and large drusen in the fellow eye. Institutional review board approval was obtained at each clinical site and written informed consent for the research was obtained from all study participants. The research was conducted under the Declaration of Helsinki and complied with the Health Portability and Accessibility Act.

Study Procedures

The AREDS2 participants were randomly assigned to placebo, lutein/zeaxanthin, docosahexaenoic acid (DHA) plus eicosapentaenoic acid (EPA), or the combination of lutein/zeaxanthin and DHA plus EPA. At baseline and annual study visits, comprehensive eye examinations were performed by certified study personnel using standardized protocols. The study visits included measurements of the best-corrected visual acuity (BCVA) using the electronic Early Treatment Diabetic Retinopathy Study (ETDRS) visual acuity charts and capture of digital stereoscopic color fundus photographs. At the second annual study visits and in the following study visits, the ancillary study of fundus autofluorescence (FAF) imaging was conducted in selected clinics. All images were acquired by technicians certified by the Fundus Photographic Reading Center at the University of Wisconsin using standard imaging protocol. Questionnaires administered at the baseline and subsequent study visits collected information that included nutrition, medications, adverse events and treatment compliance. Telephone calls were performed twice in the first year following randomization and annually thereafter to collect information about adverse events, treatment for AMD, and incidence of cataract surgery between study visits.

Image analysis

The digital stereoscopic color fundus photographs were graded centrally by certified graders, with no access to the clinical information, at the Fundus Photographic Reading Center at the University of Wisconsin (5). Calibrated stereoscopic images were viewed in a standardized digital viewing platform (ImageNet 2000, Topcon Corp, Tokyo, Japan) after color contrast and illumination adjustment. GA was defined as a lesion equal to or larger than drusen circle I-2 (diameter 433um, area $0.146mm^2$, i.e. 1/4 disc diameter and 1/16 disc area) in its widest diameter with at least two of the following features present: circular shape, sharp (well-demarcated) edges, and loss of the RPE (partial or complete depigmentation of the RPE, typically with exposure of underlying choroidal vessels).

The configuration of GA was documented, using the definitions published by Sunness et al (20), as either (i) small (single patch less than 1 disc area), (ii) multifocal, (iii) horseshoe or ring, (iv) solid or unifocal i (with or without central involvement) or (v) indeterminate. Planimetry tools were used to demarcate the area of GA within the AREDS grid in mm^2. If non-central, distance of the proximity of the atrophy border closest to the center was documented. In the case of multifocal GA, areas were summed to yield a single value for analysis, and the proximal edge of the closest lesion was used for proximity measurements to the fovea. Peripapillary atrophy was not included in the GA area if the margin of the peripapillary atrophy could be clearly distinguished from margin of GA. In situations where the two were indistinguishable, area of peripapillary atrophy that was within the AREDS grid was included in the GA area. Digital stereoscopic color fundus photographs were also analyzed for drusen, pigment changes and the presence of neovascular AMD, as described in AREDS Report 2 (5).

The FAF imaging protocol has been described previously (21). Images were taken by certified photographers using the Heidelberg Retina Angiograph (Heidelberg Engineering, Heidelberg, Germany) and fundus cameras with autofluorescence capability. In eyes graded

positive for hypoautofluorescence (classified as a well-defined, homogenously black area with a minimum size of drusen circle I-2 in its widest diameter), a halo was defined as the presence of contiguous hyperautofluorescence surrounding at least 10% of the perimeter of the area of hypoautofluorescence.

Genotype analysis

As part of the AREDS2, 1826 participants gave consent for genotype analysis. SNPs were analyzed using a custom Illumina HumanCoreExome array, as described previously (22). The loci selected for the current report were chosen as a subset of the 34 loci previously identified in a large GWAS as containing SNPs associated with significantly altered risk of late AMD (22). In total, 18 SNPs at nine loci were included. Two SNPs at two loci were selected as these had been identified from previous studies to be associated with altered speed of GA progression (rs10490924 at *ARMS2* and rs2230199 at *C3*) (23). Two SNPs at/ near *CFI* were included given ongoing interest in the potential role of *CFI* genotype in speed of GA progression and response to lampalizumab therapy: rs17440077, the same SNP analyzed in a recent phase II trial of lampalizumab therapy (17), and rs10033900, the SNP identified in a large GWAS (22) as the lead variant at the *CFI* locus (i.e. with the smallest p value for association with late AMD). Five SNPs at *CFH* were included, given consistent evidence for the strong involvement of this locus in AMD risk, together with two SNPs at *C2*/*CFB*. Seven SNPs at four other loci (*ABCA1*, *LIPC*, *CETP* and *APOE*), all previously identified from a large GWAS (22), were also included.

Eye cohorts and statistical methods

Two eye cohorts were constructed: (i) those with eyes that had GA in one or both eyes without prior or simultaneous neovascular AMD development at their baseline visit ('prevalence cohort'); (ii) those with eyes that developed GA without prior or simultaneous neovascular AMD during follow-up ('incidence cohort'). In some analyses, these two cohorts were combined to produce a third cohort ('combined cohort'). Prior or simultaneous neovascular AMD was judged positive by a history of treatment for neovascular AMD or the presence of at least two of the following features: serous detachment of the sensory retina, hemorrhage, retinal pigment epithelial detachment, fibrous tissue or hard exudates.

Kaplan-Meier analysis was performed (with eye as the unit of analysis) separately for the development of GA, progression of non-central to central GA, and progression from GA to neovascular AMD.

Mixed-model regression was performed with square root of GA area over time as the primary outcome measure (using eye as the unit of analysis), according to (i) clinical/ imaging characteristics and, separately, (ii) genotype. For these analyses, eyes were included if they had at least two visits with GA without simultaneous or prior neovascular AMD.

The square root transformation was used as this reduces the association of enlargement with baseline lesion size (24). However, regression analyses, adjusting for baseline lesion size, were also performed separately without square root transformation for comparison. In addition, regression analyses were performed separately for the (i) prevalence cohort, (ii) incidence cohort and (iii) combined cohort. The mixed-model regression analyses were

performed using adjusted repeated measures regression with the variable of interest (i.e. one at a time), years from GA first appearance, and their interaction term.

To account for the correlation of measures between visits of the same eye, we specified a first-order autoregressive covariance structure (AR(1)).

The analyses based on square root of GA area were adjusted for the square root of GA area at first appearance of GA, as well as for age and sex. Similarly, the analyses based on untransformed GA area were adjusted for GA area at first appearance of GA, as well as for age and sex. The clinical/imaging characteristics examined were defined at first appearance of GA on color photographs: GA central involvement; GA size; GA configuration; AREDS2 treatment group; DHA/EPA supplementation; lutein/zeaxanthin supplementation; smoking status; number of eyes with GA (i.e. unilateral or bilateral GA, defined as bilateral if GA was present in both eyes at any time during follow-up); presence of halo hyperautofluorescence (only assessed for the subset of eyes with hypoautofluorescence on FAF imaging). The genetic characteristics examined were participant genotype at the 18 SNPs described above. Bonferroni correction was performed to adjust for multiple testing, such that the significance level was set at p=0.002 (0.05/27).

Multivariable analysis of square root of GA area was performed using the combined cohort, with inclusion as covariates the clinical/imaging characteristics that met Bonferroni significance in the previous mixed-model regression, together with age and sex (which were chosen to remain in all models). Results were adjusted for the square root of GA area at first appearance of GA. Further multivariable models were constructed with the addition as covariates those SNPs that met Bonferroni significance in the previous mixed-model regression, with each SNP analyzed separately.

Additional analysis was performed to examine potential genetic differences between eyes with central versus non-central GA at first appearance of GA. This analysis was restricted to eyes that developed GA during follow-up (i.e. incident GA) and to participants with genetic information available. Chi-square analysis was performed using the same 18 SNPs at nine loci described above.

BCVA data were analyzed, including calculation of mean and standard deviation according to clinical/imaging characteristics and time-point. In addition, mixed-model regression of BCVA was performed in the combined cohort, with inclusion as covariates the same clinical/imaging characteristics described above.

All analyses were performed with commercially available statistical software (SAS version 9.4; SAS Institute, Cary, North Carolina, USA).

Results

Prevalent geographic atrophy

The AREDS2 included 4203 participants with annual color fundus photographs over 5 years. Of these, 517 (6.2%) eyes of 411 (9.8%) participants had GA at their baseline visit without simultaneous or prior neovascular AMD (prevalence cohort). The demographic

characteristics of this cohort at their baseline visit are shown in Table 1. Mean patient age was 76 years (SD 7 years) and 56% were female. The clinical characteristics of these eyes are shown in Table 2. At baseline, mean BCVA was 68 letters (Snellen equivalent of 20/50; SD 20 letters), mean size of GA lesion was 3.4 mm^2 (SD 4.2 mm^2), i.e. 1.3 disc areas (SD 1.6 disc areas) and mean proximity of lesion to the central macula was 413 μm (SD 467 μm). The proportions of eyes with non-central and central GA were 67% and 33%, respectively. The mean VA of eyes with non-central GA and central GA were 75 (Snellen equivalent of 20/30; SD 13 letters) and 53 letters (20/100; SD 25 letters), respectively (Table 2).

The mean follow-up period for participants where GA was present in at least one eye at the baseline visit was 4.2 years (SD 1.5; IQR 1.2). The Kaplan-Meier plot for the development of neovascular AMD in these eyes is shown in Figure 1. The 2-year rate of neovascular AMD was 8.2% and the 5-year rate was 23%.

For the 293 participants (and 348 eyes) with non-central GA in at least one eye at baseline, mean follow-up time was 4.2 years (SD 1.5; IQR 1.2). The Kaplan-Meier plot for the progression from non-central to central GA in these eyes is shown in Figure 2. The 2-year rate of progression to central GA was 22% and the 5-year rate was 60%.

Incident geographic atrophy

There were 6530 eyes of 3995 participants without GA (or simultaneous/prior neovascular AMD) at their baseline visit. The mean follow-up time for these participants was 4.4 years (SD 1.3; IQR 0.8). During this period, the number that developed new GA without prior or simultaneous neovascular AMD was 1099 (17%) eyes of 883 (22%) people (incidence cohort). The Kaplan-Meier plot for incident GA in these eyes is shown in Figure 3A, with a 19% 5-year rate of incident GA.

The demographic characteristics of this cohort were similar to those of the prevalence cohort: mean age was 74 years (SD 7 years) and 58% were female (Table 1). The clinical characteristics of these eyes are shown in Table 2. At first visit with GA, mean BCVA was 75 letters (Snellen equivalent of 20/32; SD 13 letters), mean size of GA lesion was 1.7 mm^2 (SD 2.5 mm^2), i.e. 0.7 disc areas (SD 1.0 disc areas), and mean proximity of lesion to the central macula was 459 μm (SD 513 μm). The proportions of eyes with non-central and central GA (at first visit with GA) were similar to those of the prevalence cohort, at 67% and 33%, respectively. The mean VA score of eyes with non-central GA and central GA (at first visit with GA) were 78 letters (20/30; SD 10 letters) and 70 letters (20/40; SD 16), respectively (Table 2).

Another point of interest has been the rate of GA development in the study eye when the fellow eye has neovascular AMD. This is demonstrated in Figure 3B, which shows that the incidence of GA is similar irrespective of the presence or absence of neovascular disease in the fellow eye (at the time of first appearance of the GA, or any time prior).

The Kaplan-Meier plot for the development of neovascular AMD in eyes with incident GA is shown in Figure 4. Overall, the 2-year rate of new neovascular AMD in these eyes with incident GA was 14%, and the 4-year rate was 29%. The same analysis was performed

according to the presence or absence of neovascular AMD in the fellow eye (at the time of first appearance of the GA, or any time prior). These Kaplan-Meier plots are also shown in Figure 4. The 4-year rate of neovascular AMD was substantially higher when the fellow eye status was positive (76%) versus negative (54%).

For the 628 participants (and 734 eyes) whose incident GA was non-central GA at its first appearance, mean follow-up time was 4.7 years (SD 0.8; IQR 0.7). The Kaplan-Meier plot for the progression from non-central to central GA in these eyes is shown in Figure 5, with a 32% 2-year rate and a 57% 4-year rate of progression to central GA.

Associations of various baseline characteristics and participant genotype with GA enlargement

In the prevalence cohort, the change over time in square root of GA area was 0.29 mm/year (95% CI 0.27–0.30), i.e. 0.17 disc diameters/year, or (without square root transformation) 1.42 mm^2/year (1.33–1.52), i.e. 0.61 disc areas/year. For the incidence cohort, the equivalent rates were 0.28 mm/year (0.27–0.30), i.e. 0.16 disc diameters/year, and 1.12 mm^2/year (1.04–1.19), i.e. 0.48 disc areas/year. Since enlargement rates using the square root transformation (24) were not different between the two cohorts, the cohorts were combined for subsequent regression analyses, though regression analyses were also performed separately for each cohort (for assessment of possible heterogeneity; Tables S1–2). The untransformed enlargement rates are different because the lesions at baseline are larger in the prevalence cohort.

Mixed-model regression was performed using the combined cohort for GA enlargement rates according to baseline clinical/imaging characteristics (Table 3) and participant genotype (Table 4), with adjustment for age, sex and baseline GA size. For clinical/imaging characteristics, statistically significant interactions between the square root of GA area and time (i.e. GA enlargement rate) were observed for GA central involvement at first appearance (p<0.0001), GA lesion size at first appearance (p<0.0001), GA configuration at first appearance (p<0.0001), GA affecting one or both eyes (at any point during follow-up; p<0.0001), but not for AREDS2 treatment (p=0.33), DHA/EPA supplementation (p=0.41), lutein/zeaxanthin supplementation (p=0.77) or presence of halo hyperfluorescence on FAF at first appearance (p=0.13); for smoking status, the interaction (p=0.05) was borderline significant at the nominal level but not after Bonferroni correction. For most of these characteristics, similar p values for potential interactions were observed considering the combined (Table 3), prevalent (Supplementary Table S1) and incident (Supplementary Table S2) cohorts separately and considering the enlargement rate with and without square root transformation, except for the results for smoking status and halo hyperfluorescence on FAF. In the case of smoking status, p values for potential interactions in the combined cohort were 0.05 (square root of GA area) and 0.0003 (untransformed GA area). This suggests that differences in GA enlargement rate according to smoking status may relate partly to differences in baseline lesion size. In the case of halo hyperfluorescence, p values for interactions in the combined cohort were 0.13 (square root of GA area) and <0.0001 (GA

area). Again, this suggests that differences in GA enlargement rate according to halo hyperautofluorescence may relate partly to baseline lesion size, as discussed below.

GA enlargement was significantly faster for non-central than for central GA at 0.31 mm/year (0.30–0.33) and 0.22 mm/year (0.20–0.24), respectively. Despite use of the square root transformation, some residual dependence of enlargement on baseline lesion size was observed: fastest enlargement was found with intermediate baseline lesion size of ≥0.75/<1.5 disc areas at 0.35 mm/year (0.32–0.39), while slowest enlargement was observed with large baseline lesion size of ≥4 disc areas at 0.21 mm/year (0.16–0.26). Enlargement was significantly faster for multifocal GA at 0.36 mm/year (0.34–0.39) than for small (0.26, 0.24–0.28), horseshoe/ring (0.27, 0.22–0.31) and solid/unifocal (0.24, 0.21–0.26) GA configurations. In addition, enlargement was significantly faster for bilateral GA than for unilateral GA at 0.31 mm/year (0.30–0.33) and 0.23 mm/year (0.21–0.24), respectively. Enlargement was numerically but non-significantly faster with current smoking than former smoking and never smoked statuses at 0.33 mm/year (0.29–0.37), 0.28 mm/year (0.27–0.30) and 0.27 mm/year (0.26–0.29), respectively.

GA enlargement was also analyzed according to the presence or absence of neovascular AMD in the fellow eye (at the time of GA, or prior). No significant difference was observed (Supplementary Table 3).

Supplementary analysis of square root transformation

In order to evaluate the dependence of GA enlargement, with and without square root transformation, on baseline lesion size, results for GA enlargement were plotted according to baseline lesion size (with eye as the unit of analysis) (Figure S1). In the analysis without square root transformation (Figure S1 A), the sloped line of best fit demonstrates the dependence of GA enlargement on baseline lesion size. By contrast, in the analysis with square root transformation (Figure S1 B), the relatively flat line of best fit demonstrates minimal residual dependence of GA enlargement on baseline lesion size.

Genotype and GA Enlargement

Results for participant genotype were as follows (Table 4). Statistically significant interactions between square root of GA area and time (i.e. GA enlargement rate) were observed for *ARMS2* genotype (rs10490924; p<0.0001), *C3* genotype (rs2230199; p=0.0002) and *APOE* genotype (rs73036519 but not rs429358; p=0.001 and p=0.18, respectively). A borderline significant interaction was observed for *CFI* genotype (rs10033900 but not rs17440077; p=0.004 and p=0.7, respectively). Nominally significant interactions not meeting significance by Bonferroni correction were observed for *ABCA1* genotype (rs2740488; p=0.03) and *LIPC* genotype (rs2070895 but not rs2043085; p=0.05 and p=0.12, respectively). No significant interactions were observed for *CFH* genotype, *C2/CFB* genotype or *CETP* genotype.

The change in square root of GA area over time was significantly faster in the presence of at least one versus no risk alleles at *ARMS2*, at 0.23 mm/year (0.20–0.26), 0.31 mm/year (0.28–0.33) and 0.32 mm/year (0.28–0.35) for zero (GG), one (GT) and two (TT) risk

alleles, respectively. By contrast, enlargement was significantly slower in the presence of two versus fewer risk alleles at *C3*, at 0.31 mm/year (0.28–0.33), 0.27 mm/year (0.24–0.29) and 0.18 mm/year (0.13–0.24) for zero (CC), one (CG) and two (GG) risk alleles, respectively. This paradoxical finding replicates previous results (23). Enlargement was significantly faster in the presence of one versus no protective alleles at *APOE* (rs73036519), at 0.25 mm/year (0.23–0.27) and 0.32 mm/year (0.29–0.34) for zero (GG) and one (GC) protective alleles, respectively. For *CFI* genotype (rs10033900), enlargement was faster in the presence of one versus no risk alleles, at 0.24 mm/year (0.21–0.27) and 0.31 mm/year (0.28–0.33) for zero (CC) and one (CT) risk alleles, respectively.

No significant interaction was observed according to *CFH* genotype (rs1061170, i.e. Y402H polymorphism) in the combined cohort (p=0.25). Similarly, secondary analysis of the prevalence and incidence cohorts separately (Tables S4–5) revealed no significant interactions (p=0.66 and p=0.03, respectively).

Associations of GA enlargement with baseline characteristics and genotype in multivariable analyses

Multivariable analysis was performed using the combined cohort and square root of GA area. Independent variables were included as covariates if the baseline clinical/imaging characteristics met Bonferroni significance in mixed-model regression, together with age, sex, education and smoking status. All covariates that met this criterion remained significant in the multivariable analysis (Table 5A): square root of GA area at baseline (p<0.0001), GA duration (p<0.0001), unilateral or bilateral GA (p<0.0001), central involvement at first appearance (p<0.0001) and GA configuration at first appearance (p<0.0001). Smoking status (current vs never p=0.01; overall p=0.03) and education level (p=0.01) met nominal but not Bonferroni significance, while age (p=0.12) and sex (p=0.17) remained non-significant but were left in the model. The effect estimates (for the yearly change in square root of GA area) for each covariate are given in Table 5A.

Additional multivariable analysis was performed with inclusion of genotype, specifically the SNPs that met Bonferroni significance in mixed-model regression (i.e. *APOE* rs73036519, *ARMS2* rs10490924 and *C3* rs2230199, each considered separately). The effect estimates and significance levels for the interaction between SNP and square root of GA area are shown in Table 5B. All three SNPs remained significant in the multivariable analysis: *APOE* (p=0.0003), *ARMS2* (p<0.0001) and *C3* (p<0.0001).

Association of genotype with type of incident GA (central vs. non-central)

Additional analyses were performed to investigate whether genetic differences were present between eyes with incident GA that was central versus non-central at outset. Of the 532 eyes that developed incident GA during follow-up and had genetic information available, 179 eyes had incident GA that was central at outset and 353 eyes had incident GA that was non-central. Chi-square analysis was performed using the same 18 SNPs at nine loci described above. Significance was set at p=0.003 after adjustment for multiple testing by Bonferroni correction.

The results are shown in Table S6. No significant interaction was observed between genotype and proportion of eyes with central involvement at outset for any of the SNPs tested. Results for a potential interaction met the nominal but not the adjusted significance level for *CFI* (rs10033900), with p=0.02, but no consistent dose-response effect was observed according to number of alleles for this SNP.

Visual acuity data

BCVA data were analyzed for the combined cohort (Table S7). Mean BCVA was 70 letters (20/40) at first appearance of GA and, for those eyes with follow-up of at least 5 years after first appearance of GA, was 58 letters (20/80) at 5 years. As expected, GA that was central at first appearance was associated with worse baseline BCVA (mean 59 letters [20/80]) compared with non-central GA (75 letters [20/30]). Similarly, GA with larger lesion size at first appearance was generally associated with worse baseline BCVA.

Mixed-model regression was performed using the combined cohort for change over time in BCVA according to multiple parameters including GA central involvement, GA lesion size and GA lesion configuration (all at first appearance). The overall change in BCVA over time was significantly less than 0 at −2.3 letters/year (−2.6 to −2.0; p<0.0001). No significant interaction was observed according to GA central involvement (p=0.06), lesion size (p=0.22) or GA configuration (p=0.10), though decline in BCVA was numerically faster with central GA, with intermediate lesion sizes and with horseshoe/ring configuration. For GA configuration, the significance level for horseshoe/ring versus small (p=0.006) did not quite meet the Bonferroni level (p=0.002).

Discussion

The main purpose of this study was to evaluate the natural history of GA, both established (prevalent) GA and incident GA. These AREDS2 data demonstrate the relentless burden of visual impairment of GA as the visual loss is steady throughout the 5 years of follow-up. Interestingly, in both the prevalence and incidence cohorts, about one-third of the GA presented with central involvement when GA was first detected. In those with non-central GA at first detection, approximately 60% progress to involve the center of the fovea within 4 years. In addition, almost 30% of eyes with GA may also develop neovascular AMD, especially if the fellow eye has neovascular AMD. These data emphasize the burden of visual acuity loss associated with GA, a condition for which we have no effective therapies.

In this data set, with a large number of incident and prevalent cases of GA, it was possible to examine GA enlargement over time, both overall and according to multiple clinical and genetic factors, with relatively small confidence intervals. The overall mean enlargement rate is useful in understanding the normal behavior of GA. In particular, the relative similarity in transformed enlargement rates across a wide variety of lesion sizes suggests that the enlargement of GA may be monotonic for much of its life cycle. However, slower enlargement is apparent at both the beginning (small lesions) and end (large lesions) of the life cycle. We presume that enlargement is slower at the beginning because the biological mechanisms involved in lesion propagation are not yet fully established. We also presume

that enlargement is slower at the end because growth begins to slow as lesions approach the margins of the macula.

Square root transformation

Use of the square root transformation originally arose (25) from the hypothesis that, for a single circular GA lesion, the leading edge may expand at a relatively constant rate, i.e. its radius may increase over time in a relatively linear fashion. Because of the relationship between radius and area (πr^2), this enlargement would be associated with an exponential increase in area over time. Hence, in comparing enlargement rates between different GA lesions, comparison using change in area over time would artefactually suggest that large lesions grow much faster than small lesions. However, this artefact should be eliminated by using change over time in square root of area, so that enlargement can be considered at the level of increase in radius (e.g. 0.3 mm/year) rather than area (e.g. 1.2 mm^2/year). In this way, fair comparison might be possible between enlargement rates of GA lesions with different baseline size.

Following this proposal, evidence in support of this hypothesis was obtained (24, 25): the square root transformation was found to eliminate much of the dependence of enlargement rate on baseline lesion size. One effective way to examine this phenomenon is to plot (as in Figure S1): (i) enlargement in area against baseline area, i.e. untransformed data, and (ii) enlargement in square root of area against baseline square root of area, i.e. transformed data. As demonstrated in this study (Figure S1), untransformed but not transformed enlargement rates are dependent on baseline lesion size.

The importance of the square root transformation (24) is demonstrated by several aspects of our study. The results for *CFH* genotype illustrate this well. No significant effect on enlargement rate was observed for rs1061170 (the Y402H polymorphism) or for several other SNPs analyzed, including protective SNPs. However, use of untransformed data would have suggested an artefactual association between *CFH* risk alleles (e.g. at rs1061170) and slower enlargement of GA. In the untransformed data, a significant interaction was observed in the incidence cohort (p<0.0001) but not the prevalence (p=0.25) or combined (p=0.01) cohorts; in the incidence cohort, enlargement in untransformed GA area was slower with more *CFH* risk alleles (Table S4–5). Indeed, one previous study (26) using untransformed data has reported the opposite finding, i.e. significantly faster GA enlargement with *CFH* (rs1061170) risk status. This finding is likely to be artefactual and driven instead by differences in baseline lesion size. These observations demonstrate the vital importance of the square root transformation.

Similar arguments apply to our results for halo hyperfluorescence on FAF, where use of the transformation eliminated an apparent relationship with GA enlargement. Indeed, Biarnes et al (27) previously made a related finding in their Spanish study of GA, whereby FAF pattern and baseline GA area were strongly associated with each other. Mediation analysis suggested that most of the effect of FAF pattern on GA enlargement was actually caused by baseline GA area, such that FAF pattern may be a consequence (rather than a cause) of enlarging GA. However, our results for autofluorescence are limited as the number of eyes in

this subset was small and the hyperautofluorescence analysis was confined to binary assessment, i.e. halo presence/absence. Finally, the potential relationship between smoking and GA enlargement in our data was highly significant without square root transformation but only borderline nominally significant following transformation. For these reasons, we recommend GA enlargement rates are always reported with square root transformation.

Comparison with literature

Previous smaller studies have analyzed mean enlargement rates of GA (17, 23–25, 27–35). A small number of these studies analyzed and reported mean enlargement rates using the square root transformation (23, 25, 34). Using the transformation, Yehoshua et al observed a mean enlargement rate of 0.28 mm/year (0.16 disc diameters/year) (25), i.e. the same result as in the present study. In addition, Grassmann et al, also using the transformation, reported a mean enlargement rate of 0.30 mm/year (0.17 disc diameters/year) (23), i.e. again very similar to the result in the present study. This was in one of the larger studies of GA carried out to date, comprising a total of 388 participants from a combination of the Fundus Autofluorescence in AMD (FAM) study and the AREDS (23).

Previous studies have examined potential clinical and genetic factors associated with faster enlargement of GA area (23, 29, 31, 33, 35). Klein et al reported significantly faster enlargement in multifocal GA in the Beaver Dam Eye Study, as measured in 53 eyes of 32 participants (29). Using AREDS data that included 114 eyes of 114 participants, Klein et al found a nominally significantly association between faster enlargement of GA and *ARMS2* risk genotype (31). This finding was replicated by Grassmann et al, who also demonstrated significantly faster enlargement with the non-risk genotype at *C3* (23). Caire et al reported altered enlargement according to *CFH* genotype (faster enlargement with the risk variant at rs1061170 and slower enlargement with the protective variant at rs800292) and *C2*/*CFB* genotype (slower enlargement with the protective variant at rs12614 or rs641153) (26); however, significance levels were of borderline nominal significance (without accounting for multiple testing) and, as mentioned above, the absence of square root transformation likely means that these results were artefactual. Similar findings relating to *CFH* and *C2*/*CFB* were not observed in our current study (where we used the lead variants identified from the largest GWAS of AMD (22)). More recently, Schmitz-Valckenberg observed significantly faster enlargement with multifocal GA, with non-central GA and with diffuse or banded fundus autofluorescence patterns in the GAP Study (comprising 603 participants), though potential associations with genotype were not examined in this study (33).

Our findings are in line with several previous studies that reported associations between faster enlargement and several individual variables, either clinical or genetic. Our study has extended upon these studies in its positive identification of multiple factors (both clinical/ imaging features and genetic factors) in the same large dataset with long follow-up time, and in construction of multivariable models analyzing these parameters simultaneously. In addition, it is the first highly powered study to examine the potential association of *CFI* genotype with speed of progression, following the report of non-significantly faster enlargement according to CFI genotype in a phase II trial of lampalizumab therapy (17). This work may provide important steps towards the future construction of risk models that

predict GA enlargement rates for individual eyes, either in clinical trial or in clinical practice settings.

Distinction between factors associated with geographic atrophy incidence versus enlargement

An important implication of our results arises from the distinction observed between those factors involved in increased risk of incident GA versus those associated with faster enlargement of established or prevalent GA. Some factors are shared, most notably the *ARMS2* genotype, where the minor allele is associated with both increased risk of GA (22) and with faster enlargement of GA. Similarly, smoking is strongly associated with late AMD (36) and, in our data, GA enlargement appeared numerically (though non-significantly) faster in current smokers. It is interesting that factors associated with the presence of GA are not necessarily associated with increased enlargement rates of GA. *CFH* genotype, for example, is strongly associated with risk of GA (22) but appears unimportant in influencing speed of GA enlargement. Some factors apparently act in opposite directions. In particular, the minor allele at *C3* is strongly associated with risk of GA (22) but also strongly associated with slower speed of GA enlargement. As mentioned above, this paradoxical finding in our dataset replicates a similar finding observed in a previous study (23); potential explanations for these findings are discussed below. In this sense, it appears that the birth of GA (from drusen-associated atrophy and nascent GA, and/or from reticular pseudodrusen) may be fundamentally different in nature to the propagation of established GA. This distinction has important implications for the discovery of therapeutic targets chosen either to prevent the onset of GA or to slow its progression.

In summary, factors associated with higher risk of progression to late AMD (including GA) from recent bivariate analysis of AREDS and AREDS2 data are: increased age, lower education level, positive smoking status, increased baseline AMD severity and increased genetic risk score (37). By comparison, factors associated with faster GA enlargement from the current study are: lower education level, GA presence in fellow eye, GA characteristics (intermediate size, no central involvement and multifocal configuration), genetic variants (partially distinct from risk variants for incident GA), possibly positive smoking status but not age.

Potential mechanisms linking genotype and geographic atrophy enlargement

Potential mechanisms linking these genetic variants and differential GA enlargement rates are poorly understood. In the case of *ARMS2*, Occam's razor would suggest that the mechanism responsible for increased risk of late AMD is the same as that responsible for faster enlargement of GA. However, clear identification of the mechanism linking *ARMS2* genotype and AMD has proved difficult (38, 39). Strong linkage disequilibrium across the genetic region containing *ARMS2* and its neighboring gene *HTRA1* has made it difficult to attribute disease risk to one of these genes by statistical genetic analysis alone. While the *ARMS2* gene sequence is detected in primates and the AMD-associated variant is exonic, reports of protein localization in the human retina and potential protein function have been inconsistent; one suggestion is that *ARMS2* encodes a mitochondrial protein, with the AMD variant associated with altered mRNA turnover (39). In addition, recent evidence suggests

that ARMS2 may interact with the complement system; the relative absence of ARMS2 in the high risk *ARMS2* genotype is suggested to lead to impaired complement-mediated clearance of cellular debris (40). *HTRA1* is expressed in human RPE and encodes a serine protease, with the AMD variant located in the promoter region of the gene, such that the AMD variant might be associated with altered turnover of extracellular matrix. However, reports of the effects of the variant on mRNA and protein levels have been inconsistent (39). In the future, further functional analyses and induced pluripotent stem cell technology (41) may help address these questions.

In the case of *C3*, it seems necessary to invoke two separate mechanisms for the differential effect of one genetic variant on risk of late AMD versus speed of GA enlargement. This highlights the complexity of the complement system in human biology. While the traditional roles of the complement system in innate immunity include direct cell killing through the membrane attack complex, opsonization for phagocytosis, and generation of anaphylatoxins, increasing evidence demonstrates important non-canonical roles for the complement system (42), including cell survival and immune regulation. Although prolonged excess complement activation (including through the *C3* risk variant) may be responsible for early AMD through chronic local inflammation (43), it also seems likely that some degree of complement signaling in the retina may be required for photoreceptor and neuronal health (44). This 'Goldilocks principle' is demonstrated by observations from knock-out mice, where aged mice carrying *C3* knock-out have retinal abnormalities (photoreceptor loss, retinal inflammation and reduced electroretinogram) that are at least as severe as aged mice with *CFH* knock-out (45). Hence both uncontrolled C3 activation and complete absence of C3 adversely affect the ageing mouse retina (45). Related findings have been made in other mouse models, e.g. mice lacking *C3aR* and/or *C5aR* develop retinal degeneration (46) and, in a mouse model of retinitis pigmentosa, C1q has properties of a cone photoreceptor neuronal survival factor (47). These ideas may help explain the findings from our data, where the same *C3* variant can affect risk of late AMD and speed of GA enlargement in opposite directions. An alternative explanation is that the *C3* risk variant is associated with increased likelihood of neovascular AMD, and that the presence of subclinical (i.e. non-exudative) choroidal neovascular membranes (48) adjacent to GA might slow GA enlargement.

In the case of *APOE*, an allele that is protective against late AMD is associated with faster GA enlargement. Again, it may therefore be necessary to invoke two separate mechanisms, or one mechanism with opposing effects at different stages of disease progression. APOE has antioxidant properties and, in mouse data, *APOE* deficiency is associated with abnormal retinal structure and function (49–51). On the other hand, evidence from mouse models has demonstrated that APOE can promote mononuclear phagocyte survival and chronic inflammation in the subretinal space, leading to increased photoreceptor degeneration, and that these effects are altered according to *APOE* isoform (52, 53). APOE also has important interactions with beta-amyloid, which may be implicated in AMD pathogenesis. For these reasons, it seems plausible that an *APOE* variant could have differential effects at different disease stages. Alternatively, as for *C3*, it is possible that the *APOE* protective variant is associated with decreased likelihood of neovascular AMD, and that the relative absence of subclinical choroidal neovascular membranes adjacent to GA might lead to faster GA

enlargement. It is also interesting to note that it was a different variant in *APOE* (rs73036519), i.e. one not linked with the well-known *APOE* genotypes ε2/ε3/ε4, that was associated in this study with altered speed of GA enlargement. In AREDS2 data, no effect on GA enlargement was observed according to status of *APOE* rs429358, one of two SNPs that defines ε2/ε3/ε4 genotype.

In the case of *CFH*, the data were striking for a complete absence of altered GA enlargement speed according to *CFH* genotype. Other recent analyses have shown that *CFH* genotype (at rs10922109) in AREDS2 participants had no significant effect on progression to late AMD (p=0.19), unlike *ARMS2* genotype (p=6×10⁻⁵) (37). Both sets of findings suggest that *CFH* status acts relatively early in the AMD disease process, i.e. might set the scene for the development of nascent GA (through the long-term formation of drusen and RPE abnormalities) but may not have any subsequent effect on the natural history of GA lesions.

Geographic atrophy central involvement

Our data suggest that genetic differences may not be responsible for determining central involvement at outset. This result may not be surprising, given previous natural history data suggesting that initial GA lesions occur at the macular site(s) where drusen evolution is most advanced (in terms of drusen size/confluence and presence of RPE abnormalities) (54). Hence, GA central involvement is strongly determined by central location of drusen, which in turn may be influenced by anatomical, other biological or perhaps simply stochastic reasons.

Visual acuity data

For completeness, we included BCVA data in this report. These data demonstrate the behavior of eyes with GA, according to GA subtype, in terms of rate of decline of BCVA over time. The absence of statistically significant interactions according to imaging/clinical characteristics of GA, in contrast to positive findings obtained using GA area as the primary outcome, demonstrates that BCVA by itself may be a poor indicator of GA progression. However, one interesting finding was the large difference between BCVA for central (mean 53 letters) and non-central GA (75 letters) at baseline in prevalent disease, versus the small difference between BCVA for central GA (70 letters) and non-central GA (78 letters) at outset in incident disease. This suggests that anatomical involvement of the fovea by GA (as judged by color fundus photography) is necessary but not sufficient for a substantial reduction in BCVA. Indeed, the data in this study further suggest that duration and hence degree of atrophy are required alongside central involvement for BCVA to be profoundly affected.

Strengths and limitations

The strengths of this study include its large size and long follow-up period. The dataset contains the largest number of eyes with GA so far in the published literature, to our knowledge. Long duration of follow-up with fixed annual imaging intervals allowed capture of incident GA in many eyes together with meaningful calculation of changes in GA area over multiple time-points. It was also possible to exclude from the analyses those eyes with simultaneous or prior neovascular AMD, in order to examine more accurately the behavior

of 'pure GA' (i.e. without any possible influence from coexistent neovascular disease and/or anti-VEGF therapy). In a similar way, it was also possible to analyze the emergence of neovascular disease from pre-existing GA, specifically in eyes without previous history of neovascular AMD. Standardized grading of GA and other imaging features by an independent reading center was a strength in this study. Furthermore, comprehensive and uniform information was collected on all participants, which allowed analysis of GA according to participant characteristics, imaging features and (in a large subset of participants) AMD genotype.

Potential limitations included the use of color fundus photography as the main imaging modality for the assessment of GA, since GA is thought to be detected earlier, and perhaps with less variability of GA area measurement, on FAF and optical coherence tomography (OCT) (21). Future studies may prove OCT to be a more sensitive and reproducible approach, and definitions for atrophy of OCT have recently been proposed (55). However, previous studies have demonstrated high correlation between color fundus photography and FAF in the measurement of GA area and progression (17, 21, 56). Further limitations included the completeness of genotype data (which was available in 1826 of the 4203 AREDS2 participants), the retrospective (unplanned) nature of the analysis and the absence of data on some suggested risk factors for GA progression (e.g. those obtained from OCT (57), such as choroidal thickness, border type and outer retinal tubulation, as well as data on reticular pseudodrusen).

Conclusions

Data from the AREDS2 have provided a large and comprehensive body of information on the incidence, clinical characteristics and behavior of GA in AMD. This includes analysis of potential factors associated with altered speed of progression. These data are useful for our understanding of natural history and may also provide insights into the pathogenesis and potential treatment of GA, whether incident or established. These data are also important for both endpoint selection and the recruitment and stratification of participants into clinical trials for treatment aimed at stopping or slowing GA enlargement. Selection of eyes with prospective knowledge of patient genotype and specific imaging features would be ideal, where those eyes with highest risk of rapid enlargement would be most suitable for inclusion. The results may also have implications for further study of potential interactions between specific AMD genotypes and differential response to individual therapies.

Supplementary Material

Refer to Web version on PubMed Central for supplementary material.

Acknowledgments

Abbreviations

AMD	age-related macular degeneration
AREDS	Age-Related Eye Disease Study
BCA	best-corrected visual acuity
DHA	docosahexaenoic acid
EPA	eicosapentaenoic acid
ETDRS	Early Treatment Diabetic Retinopathy Study
FAM	Fundus Autofluorescence in AMD
FAF	fundus autofluorescence
FDA	Food and Drug Administration
GA	geographic atrophy
GWAS	genome-wide association study
IQR	interquartile range
OCT	optical coherence tomography
RPE	retinal pigment epithelium
SD	standard deviation
SNP	single nucleotide polymorphism

References

1. Gass JD. Drusen and disciform macular detachment and degeneration. Arch Ophthalmol. 1973;90(3):206–17. [PubMed: 4738143]

2. Schmitz-Valckenberg S, Sadda S, Staurenghi G, Chew EY, Fleckenstein M, Holz FG, et al. GEOGRAPHIC ATROPHY: Semantic Considerations and Literature Review. Retina. 2016;36(12): 2250–64. [PubMed: 27552292]

3. Bird AC, Phillips RL, Hageman GS. Geographic atrophy: a histopathological assessment. JAMA Ophthalmol. 2014;132(3):338–45. [PubMed: 24626824]

4. AREDS RG. The Age-Related Eye Disease Study system for classifying age-related macular degeneration from stereoscopic color fundus photographs: the Age-Related Eye Disease Study Report Number 6. Am J Ophthalmol. 2001;132(5):668–81. [PubMed: 11704028]

5. Danis RP, Domalpally A, Chew EY, Clemons TE, Armstrong J, SanGiovanni JP, et al. Methods and reproducibility of grading optimized digital color fundus photographs in the Age-Related Eye Disease Study 2 (AREDS2 Report Number 2). Invest Ophthalmol Vis Sci 2013;54(7):4548–54. [PubMed: 23620429]

6. Danis RP, Lavine JA, Domalpally A. Geographic atrophy in patients with advanced dry age-related macular degeneration: current challenges and future prospects. Clin Ophthalmol. 2015;9:2159–74. [PubMed: 26640366]

7. Sunness JS. Face Fields and Microperimetry for Estimating the Location of Fixation in Eyes with Macular Disease. J Vis Impair Blind. 2008;102(11):679–89. [PubMed: 20585406]

8. Rudnicka AR, Jarrar Z, Wormald R, Cook DG, Fletcher A, Owen CG. Age and gender variations in age-related macular degeneration prevalence in populations of European ancestry: a meta-analysis. Ophthalmology. 2012;119(3):571–80. [PubMed: 22176800]

9. A Study Investigating the Efficacy and Safety of Lampalizumab Intravitreal Injections in Participants With Geographic Atrophy Secondary to Age-Related Macular Degeneration. https://ClinicalTrials.gov/show/NCT02247479.

10. A Study Investigating the Safety and Efficacy of Lampalizumab Intravitreal Injections in Participants With Geographic Atrophy Secondary to Age-Related Macular Degeneration. https://ClinicalTrials.gov/show/NCT02247531.

11. Study of of APL-2 Therapy in Patients Geographic Atrophy. https://ClinicalTrials.gov/show/NCT02503332.

12. Csaky K, Ferris F, 3rd, Chew EY, Nair P, Cheetham JK, Duncan JL. Report From the NEI/FDA Endpoints Workshop on Age-Related Macular Degeneration and Inherited Retinal Diseases. Invest Ophthalmol Vis Sci. 2017;58(9):3456–63. [PubMed: 28702674]

13. Holz FG, Sadda SR, Staurenghi G, Lindner M, Bird AC, Blodi BA, et al. Imaging Protocols in Clinical Studies in Advanced Age-Related Macular Degeneration: Recommendations from Classification of Atrophy Consensus Meetings. Ophthalmology. 2017;124(4):464–78. [PubMed: 28109563]

14. Sadda SR, Chakravarthy U, Birch DG, Staurenghi G, Henry EC, Brittain C. Clinical Endpoints for the Study of Geographic Atrophy Secondary to Age-Related Macular Degeneration. Retina. 2016;36(10):1806–22. [PubMed: 27652913]

15. Schaal KB, Rosenfeld PJ, Gregori G, Yehoshua Z, Feuer WJ. Anatomic Clinical Trial Endpoints for Nonexudative Age-Related Macular Degeneration. Ophthalmology. 2016;123(5):1060–79. [PubMed: 26952592]

16. Yehoshua Z, Rosenfeld PJ, Albini TA. Current Clinical Trials in Dry AMD and the Definition of Appropriate Clinical Outcome Measures. Semin Ophthalmol. 2011;26(3):167–80.

17. Yaspan BL, Williams DF, Holz FG, Regillo CD, Li Z, Dressen A, et al. Targeting factor D of the alternative complement pathway reduces geographic atrophy progression secondary to age-related macular degeneration. Sci Transl Med. 2017;9(395).

18. Yehoshua Z, de Amorim Garcia Filho CA, Nunes RP, Gregori G, Penha FM, Moshfeghi AA, et al. Association Between Growth of Geographic Atrophy and the Complement Factor I Locus. Ophthalmic Surg Lasers Imaging Retina. 2015;46(7):772–4. [PubMed: 26247461]

19. Group AR, Chew EY, Clemons T, SanGiovanni JP, Danis R, Domalpally A, et al. The Age-Related Eye Disease Study 2 (AREDS2): study design and baseline characteristics (AREDS2 report number 1). Ophthalmology. 2012;119(11):2282–9. [PubMed: 22840421]

20. Sunness JS, Bressler NM, Tian Y, Alexander J, Applegate CA. Measuring geographic atrophy in advanced age-related macular degeneration. Invest Ophthalmol Vis Sci. 1999;40(8):1761–9. [PubMed: 10393046]

21. Domalpally A, Danis R, Agron E, Blodi B, Clemons T, Chew E, et al. Evaluation of Geographic Atrophy from Color Photographs and Fundus Autofluorescence Images: Age-Related Eye Disease Study 2 Report Number 11. Ophthalmology. 2016;123(11):2401–7. [PubMed: 27448832]

22. Fritsche LG, Igl W, Bailey JN, Grassmann F, Sengupta S, Bragg-Gresham JL, et al. A large genome-wide association study of age-related macular degeneration highlights contributions of rare and common variants. Nat Genet. 2016;48(2):134–43. [PubMed: 26691988]

23. Grassmann F, Fleckenstein M, Chew EY, Strunz T, Schmitz-Valckenberg S, Gobel AP, et al. Clinical and genetic factors associated with progression of geographic atrophy lesions in age-related macular degeneration. PLoS One. 2015;10(5):e0126636. [PubMed: 25962167]

24. Feuer WJ, Yehoshua Z, Gregori G, Penha FM, Chew EY, Ferris FL, et al. Square root transformation of geographic atrophy area measurements to eliminate dependence of growth rates

on baseline lesion measurements: a reanalysis of age-related eye disease study report no. 26. JAMA Ophthalmol. 2013;131(1):110–1. [PubMed: 23307222]

25. Yehoshua Z, Rosenfeld PJ, Gregori G, Feuer WJ, Falcao M, Lujan BJ, et al. Progression of geographic atrophy in age-related macular degeneration imaged with spectral domain optical coherence tomography. Ophthalmology. 2011;118(4):679–86. [PubMed: 21035861]

26. Caire J, Recalde S, Velazquez-Villoria A, Garcia-Garcia L, Reiter N, Anter J, et al. Growth of geographic atrophy on fundus autofluorescence and polymorphisms of CFH, CFB, C3, FHR1–3, and ARMS2 in age-related macular degeneration. JAMA Ophthalmol. 2014;132(5):528–34. [PubMed: 24557084]

27. Biarnes M, Arias L, Alonso J, Garcia M, Hijano M, Rodriguez A, et al. Increased Fundus Autofluorescence and Progression of Geographic Atrophy Secondary to Age-Related Macular Degeneration: The GAIN Study. Am J Ophthalmol. 2015;160(2):345–53 e5. [PubMed: 25982972]

28. Sunness JS, Margalit E, Srikumaran D, Applegate CA, Tian Y, Perry D, et al. The long-term natural history of geographic atrophy from age-related macular degeneration: enlargement of atrophy and implications for interventional clinical trials. Ophthalmology. 2007;114(2):271–7. [PubMed: 17270676]

29. Klein R, Meuer SM, Knudtson MD, Klein BE. The epidemiology of progression of pure geographic atrophy: the Beaver Dam Eye Study. Am J Ophthalmol. 2008;146(5):692–9. [PubMed: 18672224]

30. Lindblad AS, Lloyd PC, Clemons TE, Gensler GR, Ferris FL, 3rd, Klein ML, et al. Change in area of geographic atrophy in the Age-Related Eye Disease Study: AREDS report number 26. Arch Ophthalmol. 2009;127(9):1168–74. [PubMed: 19752426]

31. Klein ML, Ferris FL, 3rd, Francis PJ, Lindblad AS, Chew EY, Hamon SC, et al. Progression of geographic atrophy and genotype in age-related macular degeneration. Ophthalmology. 2010;117(8):1554–9, 9 e1. [PubMed: 20381870]

32. Joachim N, Mitchell P, Kifley A, Rochtchina E, Hong T, Wang JJ. Incidence and progression of geographic atrophy: observations from a population-based cohort. Ophthalmology. 2013;120(10): 2042–50 [PubMed: 23706948]

33. Schmitz-Valckenberg S, Sahel JA, Danis R, Fleckenstein M, Jaffe GJ, Wolf S, et al. Natural History of Geographic Atrophy Progression Secondary to Age-Related Macular Degeneration (Geographic Atrophy Progression Study). Ophthalmology. 2016;123(2):361–8. [PubMed: 26545317]

34. Yehoshua Z, de Amorim Garcia Filho CA, Nunes RP, Gregori G, Penha FM, Moshfeghi AA, et al. Systemic complement inhibition with eculizumab for geographic atrophy in age-related macular degeneration: the COMPLETE study. Ophthalmology. 2014;121(3):693–701. [PubMed: 24289920]

35. Holz FG, Bindewald-Wittich A, Fleckenstein M, Dreyhaupt J, Scholl HP, Schmitz-Valckenberg S, et al. Progression of geographic atrophy and impact of fundus autofluorescence patterns in age-related macular degeneration. Am J Ophthalmol. 2007;143(3):463–72. [PubMed: 17239336]

36. Chakravarthy U, Wong TY, Fletcher A, Piault E, Evans C, Zlateva G, et al. Clinical risk factors for age-related macular degeneration: a systematic review and meta-analysis. BMC Ophthalmol. 2010;10:31. [PubMed: 21144031]

37. Ding Y, Liu Y, Yan Q, Fritsche LG, Cook RJ, Clemons T, et al. Bivariate Analysis of Age-Related Macular Degeneration Progression Using Genetic Risk Scores. Genetics. 2017;206(1):119–33. [PubMed: 28341650]

38. Swaroop A, Chew EY, Rickman CB, Abecasis GR. Unraveling a multifactorial late-onset disease: from genetic susceptibility to disease mechanisms for age-related macular degeneration. Annu Rev Genomics Hum Genet. 2009;10:19–43. [PubMed: 19405847]

39. Chromosome Wang G. 10q26 locus and age-related macular degeneration: a progress update. Exp Eye Res. 2014;119:1–7. [PubMed: 24291204]

40. Micklisch S, Lin Y, Jacob S, Karlstetter M, Dannhausen K, Dasari P, et al. Age-related macular degeneration associated polymorphism rs10490924 in ARMS2 results in deficiency of a complement activator. J Neuroinflammation. 2017;14(1):4. [PubMed: 28086806]

41. Sun S, Li Z, Glencer P, Cai B, Zhang X, Yang J, et al. Bringing the age-related macular degeneration high-risk allele age-related maculopathy susceptibility 2 into focus with stem cell technology. Stem Cell Res Ther. 2017;8(1):135. [PubMed: 28583181]

42. Calippe B, Augustin S, Beguier F, Charles-Messance H, Poupel L, Conart JB, et al. Complement Factor H Inhibits CD47-Mediated Resolution of Inflammation. Immunity. 2017;46(2):261–72. [PubMed: 28228282]

43. Anderson DH, Radeke MJ, Gallo NB, Chapin EA, Johnson PT, Curletti CR, et al. The pivotal role of the complement system in aging and age-related macular degeneration: hypothesis re-visited. Prog Retin Eye Res. 2010;29(2):95–112. [PubMed: 19961953]

44. Kawa MP, Machalinska A, Roginska D, Machalinski B. Complement system in pathogenesis of AMD: dual player in degeneration and protection of retinal tissue. J Immunol Res. 2014;2014:483960. [PubMed: 25276841]

45. Hoh Kam J, Lenassi E, Malik TH, Pickering MC, Jeffery G. Complement component C3 plays a critical role in protecting the aging retina in a murine model of age-related macular degeneration. Am J Pathol. 2013;183(2):480–92. [PubMed: 23747511]

46. Yu M, Zou W, Peachey NS, McIntyre TM, Liu J. A novel role of complement in retinal degeneration. Invest Ophthalmol Vis Sci. 2012;53(12):7684–92. [PubMed: 23074214]

47. Humphries MM, Kenna PF, Campbell M, Tam LC, Nguyen AT, Farrar GJ, et al. C1q enhances cone photoreceptor survival in a mouse model of autosomal recessive retinitis pigmentosa. Eur J Hum Genet. 2012;20(1):64–8. [PubMed: 21863053]

48. Roisman L, Zhang Q, Wang RK, Gregori G, Zhang A, Chen CL, et al. Optical Coherence Tomography Angiography of Asymptomatic Neovascularization in Intermediate Age-Related Macular Degeneration. Ophthalmology. 2016;123(6):1309–19. [PubMed: 26876696]

49. Ong JM, Zorapapel NC, Rich KA, Wagstaff RE, Lambert RW, Rosenberg SE, et al. Effects of cholesterol and apolipoprotein E on retinal abnormalities in ApoE-deficient mice. Invest Ophthalmol Vis Sci. 2001;42(8):1891–900. [PubMed: 11431458]

50. Ong JM, Zorapapel NC, Aoki AM, Brown DJ, Nesburn AB, Rich KA, et al. Impaired electroretinogram (ERG) response in apolipoprotein E-deficient mice. Curr Eye Res. 2003;27(1):15–24. [PubMed: 12868005]

51. Dithmar S, Curcio CA, Le NA, Brown S, Grossniklaus HE. Ultrastructural changes in Bruch's membrane of apolipoprotein E-deficient mice. Invest Ophthalmol Vis Sci. 2000;41(8):2035–42. [PubMed: 10892840]

52. Levy O, Calippe B, Lavalette S, Hu SJ, Raoul W, Dominguez E, et al. Apolipoprotein E promotes subretinal mononuclear phagocyte survival and chronic inflammation in age-related macular degeneration. EMBO Mol Med. 2015;7(2):211–26. [PubMed: 25604058]

53. Levy O, Lavalette S, Hu SJ, Housset M, Raoul W, Eandi C, et al. APOE Isoforms Control Pathogenic Subretinal Inflammation in Age-Related Macular Degeneration. J Neurosci. 2015;35(40):13568–76. [PubMed: 26446211]

54. Klein ML, Ferris FL, 3rd, Armstrong J, Hwang TS, Chew EY, Bressler SB, et al. Retinal precursors and the development of geographic atrophy in age-related macular degeneration. Ophthalmology. 2008;115(6):1026–31. [PubMed: 17981333]

55. Sadda SR, Guymer R, Holz FG, Schmitz-Valckenberg S, Curcio CA, Bird AC, et al. Consensus Definition for Atrophy Associated with Age-Related Macular Degeneration on OCT: Classification of Atrophy Report 3. Ophthalmology. 2017.

56. Khanifar AA, Lederer DE, Ghodasra JH, Stinnett SS, Lee JJ, Cousins SW, et al. Comparison of color fundus photographs and fundus autofluorescence images in measuring geographic atrophy area. Retina. 2012;32(9):1884–91. [PubMed: 22547167]

57. Sleiman K, Veerappan M, Winter KP, McCall MN, Yiu G, Farsiu S, et al. Optical Coherence Tomography Predictors of Risk for Progression to Non-Neovascular Atrophic Age-Related Macular Degeneration. Ophthalmology. 2017.
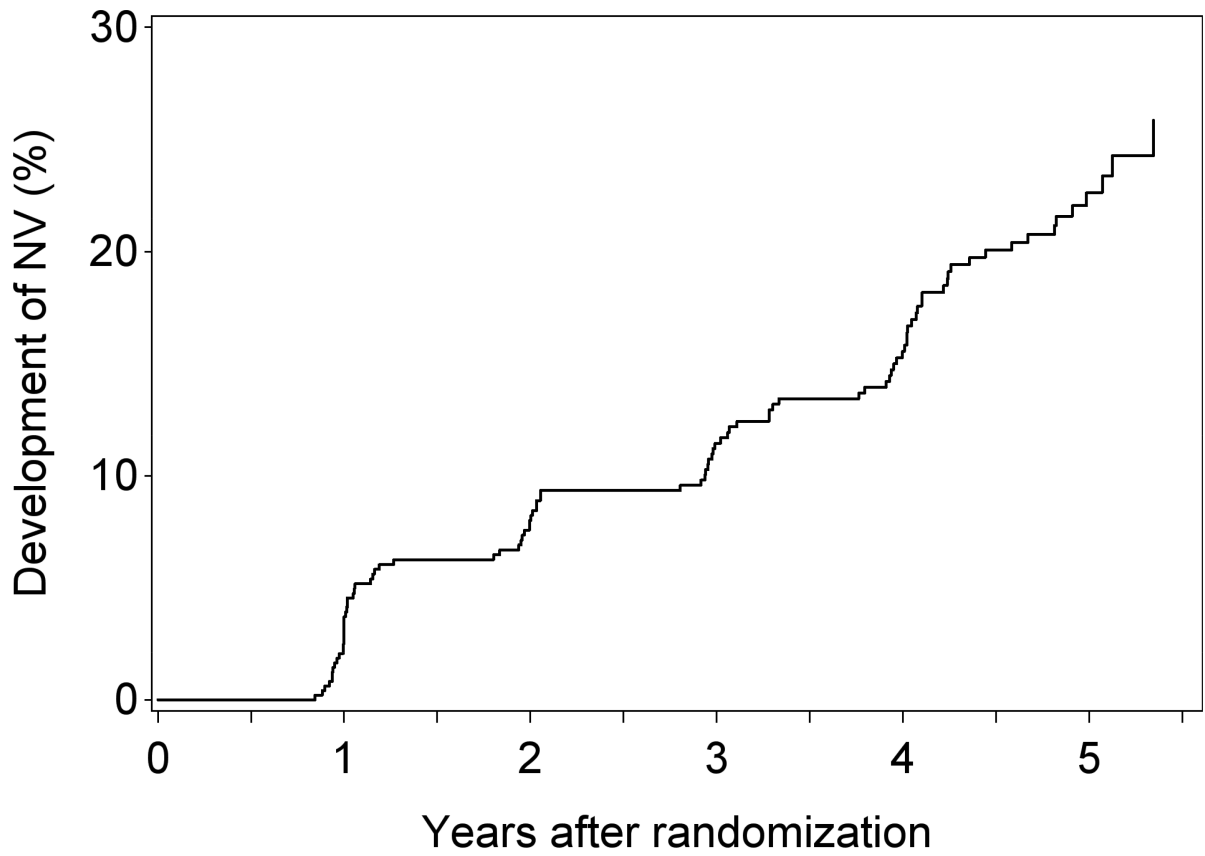
Figure 1.
Kaplan-Meier plot of the development of neovascular AMD in eyes with prevalent GA (i.e. where GA was present at baseline).
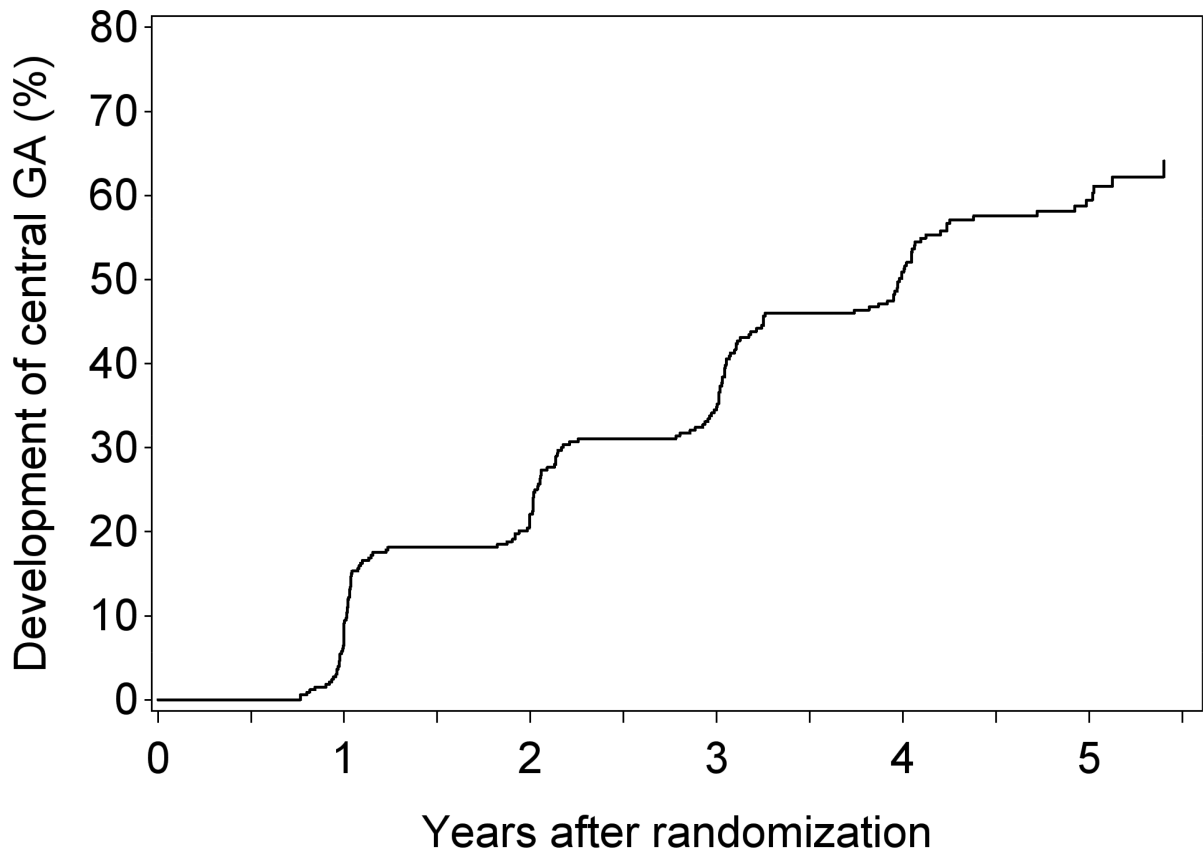
Figure 2.
Kaplan-Meier plot of the development of central GA in eyes where non-central GA was present at baseline.
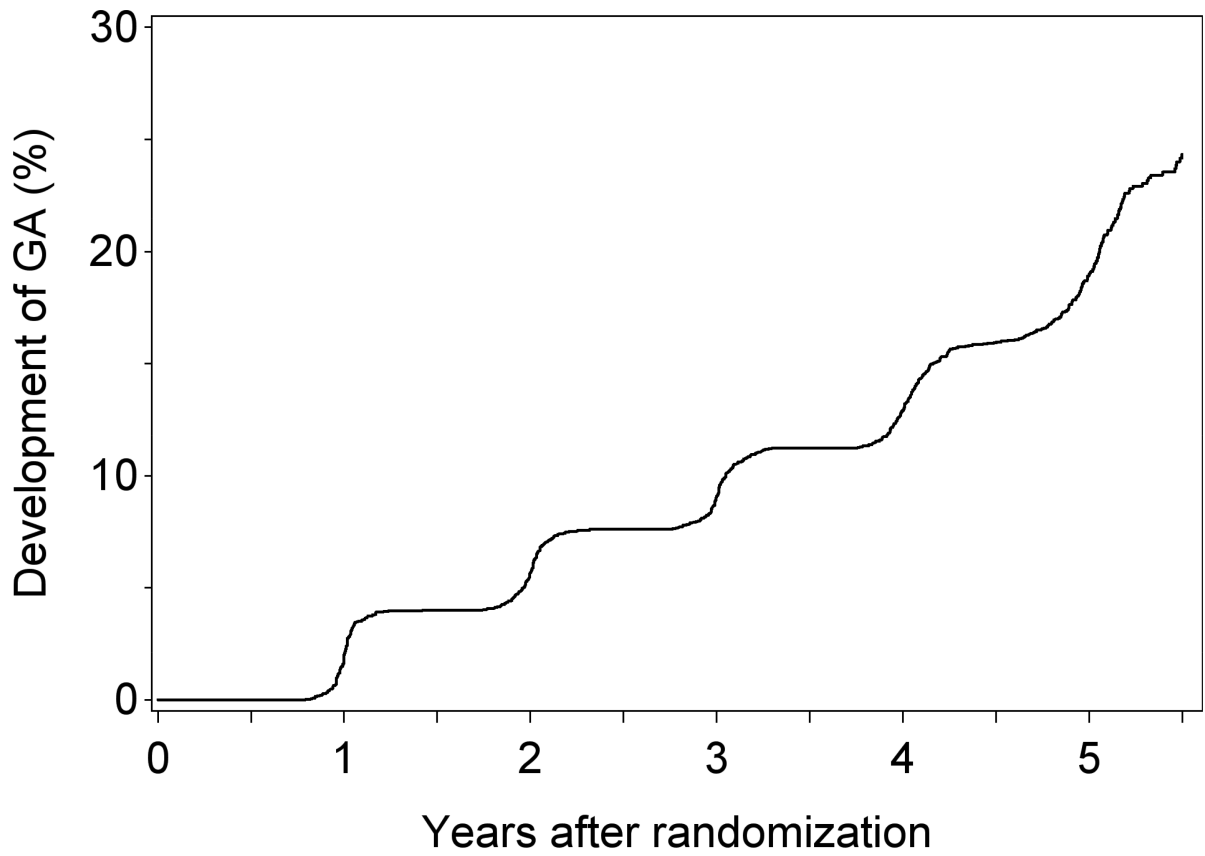
Figure 3A.
Kaplan-Meier plot of the development of GA (without simultaneous/prior neovascular AMD) in eyes that did not have GA (or neovascular AMD) at baseline (i.e. incident GA).
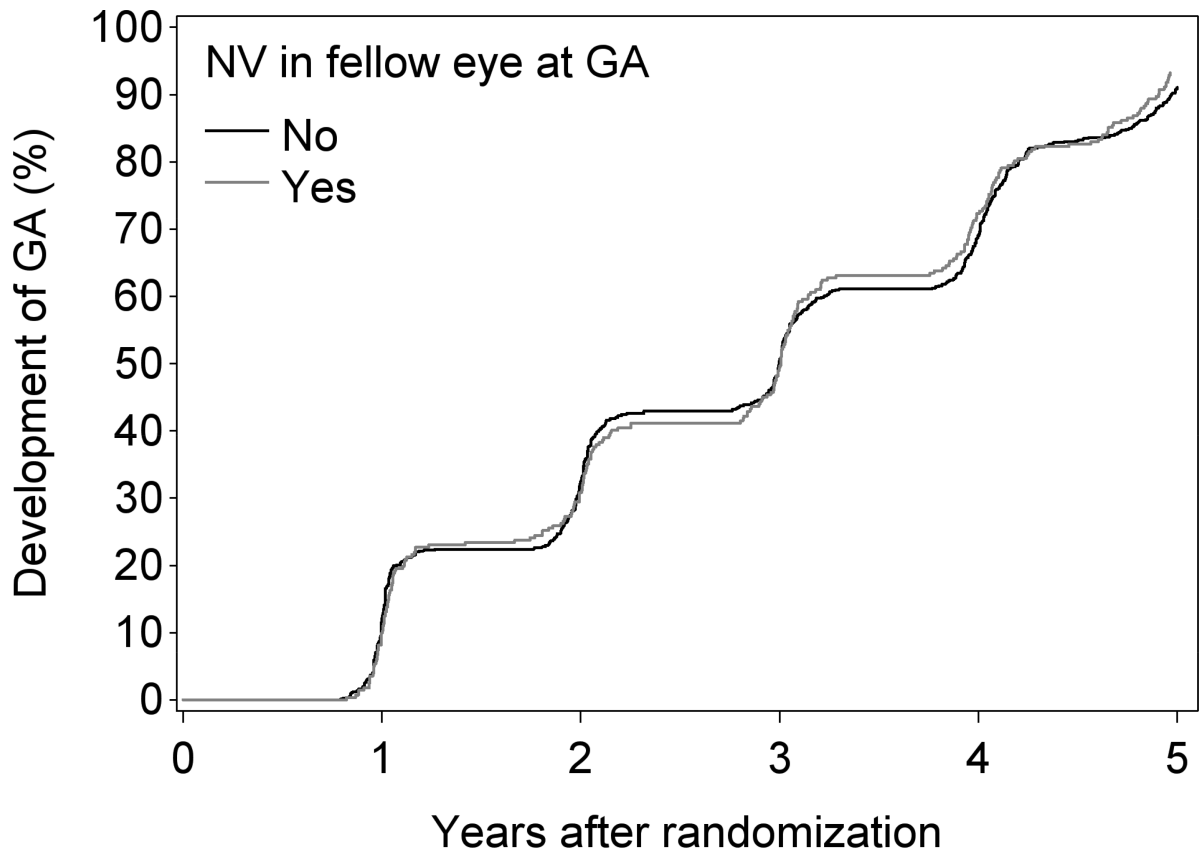
Figure 4B.
Kaplan-Meier plot of the development of GA (without simultaneous/prior neovascular AMD) in eyes according to the presence or absence of neovascular AMD in the fellow eye at the time of GA.
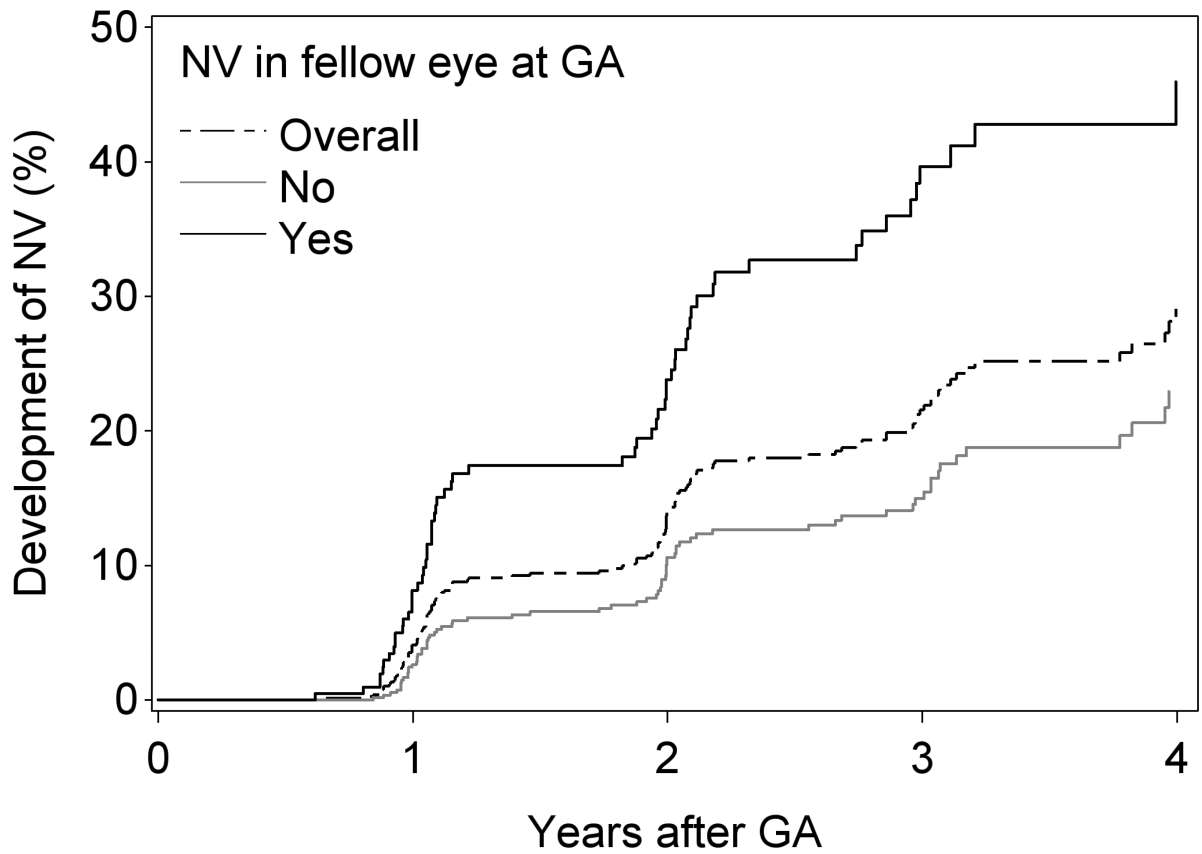
Figure 5.
Kaplan-Meier plot of the development of neovascular AMD in eyes with incident GA (i.e. where GA developed during follow-up): overall and according to the presence or absence of neovascular AMD in the fellow eye at the time of GA.
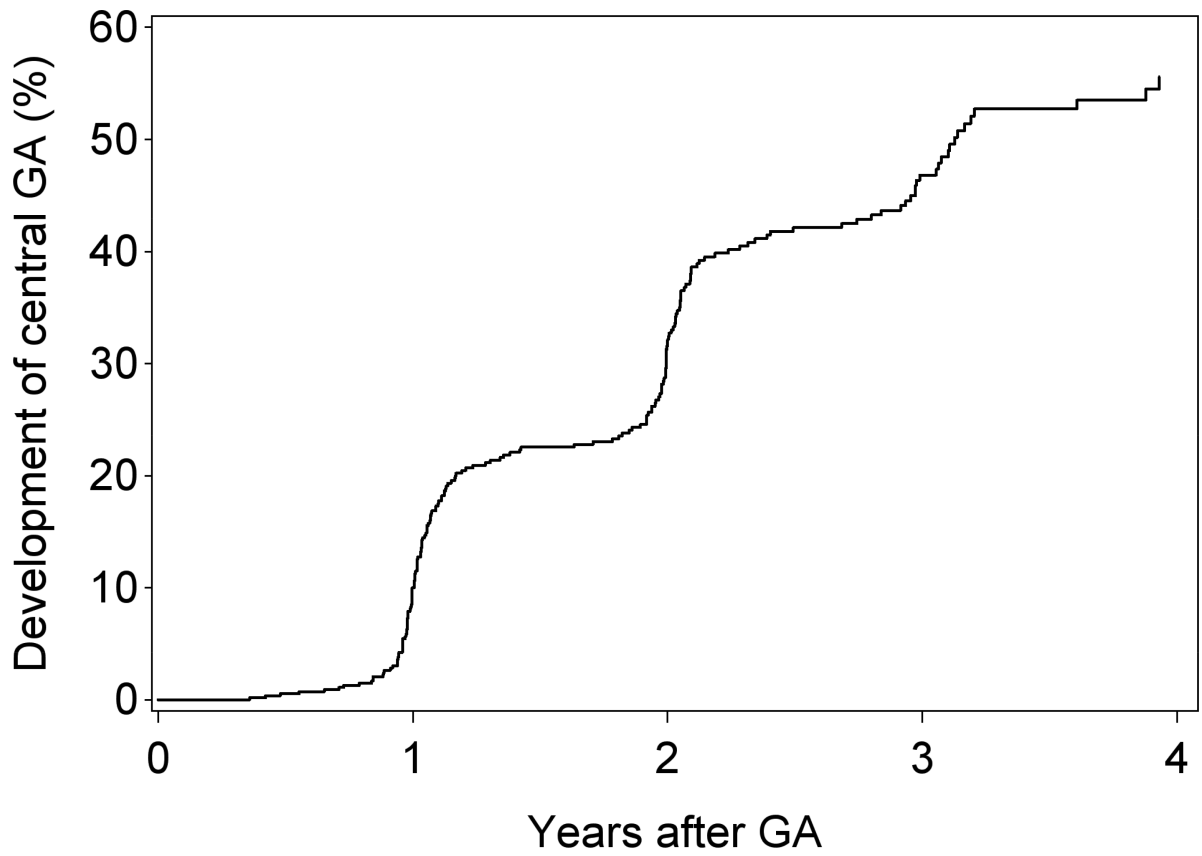
Figure 6.
Kaplan-Meier plot of the development of central GA in eyes that developed non-central GA during follow-up (i.e. incident non-central GA).

Table 1

Participant demographics at baseline, stratified by prevalent, incident, and combined cohorts

	Prevalence cohort: existing GA at baseline (without simultaneous or prior neovascular AMD)	Incidence cohort: new GA during follow-up (without simultaneous or prior neovascular AMD)	Combined cohort (combination of prevalence and incidence cohorts)
Participants	411 (517 eyes)	883 (1099 eyes)	1168 (1616 eyes)
Mean age (years)	75.8 (SD 6.8)	74.4 (SD 7.1)	74.9 (SD 7.0)
Female: n (%)	232 (56.4%)	510 (57.8%)	676 (57.9%)
Smoking status: n (%)			
Never	155 (37.7%)	364 (41.2%)	473 (40.5%)
Former	227 (55.2%)	462 (52.3%)	617 (52.8%)
Current	29 (7.1%)	57 (6.5%)	78 (6.7%)
Education level: n (%)			
Unknown	9 (2.2%)	17 (1.9%)	23 (2.0%)
High school or less	156 (38.0%)	300 (34.0%)	409 (35.0%)
At least some College	174 (42.3%)	402 (45.5%)	523 (44.8%)
Post-graduate	72 (17.5%)	164 (18.6%)	213 (18.2%)
Treatment group: n (%)			
Control	98 (23.8%)	238 (27.0%)	303 (25.9%)
Lutein/zeaxanthin	91 (22.1%)	194 (22.0%)	261 (22.3%)
DHA/EPA	104 (25.3%)	224 (25.4%)	294 (25.2%)
Combination	118 (28.7%)	227 (25.7%)	310 (26.5%)
Genotype data: n (%)			
Absent	268 (65.2%)	456 (51.6%)	652 (55.8%)
Present	143 (34.8%)	427 (48.4%)	516 (44.2%)
FAF data: n (%)			
Absent	185 (45.0%)	305 (34.5%)	828 (70.9%)
Present	226 (55.0%)	578 (65.5%)	340 (29.1%)
Mean follow-up (years)	4.2 (SD 1.5); IQR 1.2	4.7 (SD 0.8); IQR 0.8	4.5 (SD 1.1); IQR 1.0
Participants with 2 visits with GA without simultaneous or prior neovascular AMD (for inclusion in regression analyses)			
Participants	367 (456 eyes)	622 (763 eyes)	897 (1219 eyes)

SD=standard deviation; GA=geographic atrophy; AMD=age-related macular degeneration; DHA=docosahexaenoic acid; EPA=eicosapentaenoic acid; FAF=fundus autofluorescence; IQR=interquartile range (upper quartile – lower quartile)

Table 2

Characteristics of geographic atrophy at first appearance and progression to neovascular AMD and central geographic atrophy

	Prevalence cohort: existing GA at baseline (without simultaneous or prior neovascular AMD)	Incidence cohort: new GA during follow-up (without simultaneous or prior neovascular AMD)	Combined cohort (combination of prevalence and incidence cohorts)
Eyes	517	1099	1616
Mean (SD) BCVA at first appearance of GA (letters) (Snellen equivalent)			
All GA	67.5 (20.2) (20/50)	75.4 (13.0) (20/30)	69.7 (18.4) (20/40)
Central GA	53.0 (24.6) (20/100)	70.0 (15.8) (20/40)	58.8 (22.2) (20/60)
Non-central GA	74.6 (12.6) (20/30)	78.1 (10.3) (20/30)	74.9 (13.4) (20/30)
Mean (SD) size of GA at first appearance of GA (mm^2)	3.4 (4.2)	1.7 (2.5)	2.2 (3.2)
	1.3 DA (1.6 DA)	0.7 DA (1.0 DA)	0.9 DA (1.3 DA)
Mean (SD) proximity of GA to central macula at first appearance of GA (μm)	413 (467)	459 (513)	445 (499)
Eyes (%) according to central involvement at first appearance of GA			
Central GA	169 (32.7%)	365 (33.2%)	534 (33.4%)
Non-central GA	348 (67.3%)	734 (66.8%)	1082 (67.0%)
Eyes (%) according to GA area at first appearance (disc areas)			
<0.75	273 (52.8%)	845 (76.9%)	1118 (69.2%)
>=0.75 to <1.5	85 (16.4%)	142 (12.9%)	227 (14.0%)
>=1.5 to <2.0	34 (6.6%)	35 (3.2%)	69 (4.3%)
>=2.0 to <4	84 (16.2%)	59 (5.4%)	143 (8.8%)
>=4	41 (7.9%)	18 (1.6%)	59 (3.7%)
Eyes (%) according to GA configuration at first appearance			
Small (single patch <1DA)	184 (35.6%)	630 (57.3%)	814 (50.4%)
Multifocal	126 (24.4%)	271 (24.7%)	397 (24.6%)
Horseshoe or ring	44 (8.5%)	27 (2.5%)	71 (4.4%)
Solid	132 (25.5%)	150 (13.6%)	282 (17.5%)
Indeterminate	31 (6.0%)	21 (1.9%)	52 (3.2%)
Eyes (%) that developed neovascular AMD	94 (18.2%)	138 (12.6%)	232 (14.4%)
Mean (SD) time to event (years)	2.7 (1.4)	1.8 (1.0)	2.2 (1.2%)
Eyes (%) with non-central GA at first appearance that developed central GA	178 (51.2%)	203 (27.7%)	381 (35.2%)
Mean (SD) time to event (years)	2.4 (1.3)	1.7 (0.8)	2.0 (1.1)

SD=standard deviation; DA=disc areas; GA=geographic atrophy; AMD=age-related macular degeneration; DHA=docosahexaenoic acid; EPA=eicosapentaenoic acid

Table 3

Mixed models regression of square root of geographic atrophy area for combined cohort according to clinical and imaging characteristics.

		Change per year in square root of GA area [1]			Change per year in GA area [2]		
		Estimate (mm)	95% CI (mm)	p	Estimate (mm^2)	95% CI (mm^2)	p
Overall		0.28 (0.16 DD)	0.27–0.29	<0.0001	1.29 (0.55 DA)	1.23–1.35	<0.0001
Central GA at baseline	No	0.31	0.30–0.33	<0.0001	1.41	1.34–1.48	<0.0001
	Yes	0.22	0.20–0.24		1.06	0.96–1.16	
GA size (disc areas) at baseline	<0.75	0.28	0.26–0.29	<0.0001	0.97	0.90–1.04	<0.0001
	>=0.75,<1.5	0.35	0.32–0.39		1.83	1.68–1.99	
	>=1.5,<2.0	0.27	0.22–0.32		1.58	1.34–1.82	
	>=2.0,<4.0	0.28	0.24–0.31		1.92	1.75–2.08	
	>=4.0	0.21	0.16–0.26		1.92	1.67–2.17	
Configuration at baseline	Small	0.26	0.24–0.28	<0.0001	0.89	0.81–0.98	<0.0001
	Multifocal	0.36	0.34–0.39		1.66	1.54–1.77	
	Horseshoe/ring	0.27	0.22–0.31		1.99	1.77–2.22	
	Solid	0.24	0.21–0.26		1.34	1.22–1.47	
	Indeterminate	0.37	0.31–0.42		2.37	2.08–2.66	
AREDS2 treatment	Control	0.27	0.25–0.29	0.33	1.27	1.15–1.39	0.89
	L/Z	0.29	0.26–0.31		1.31	1.18–1.44	
	DHA/EPA	0.30	0.28–0.32		1.32	1.21–1.44	
	Combination	0.28	0.26–0.30		1.27	1.16–1.38	
DHA/EPA main effect	No	0.28	0.26–0.29	0.41	1.29	1.20–1.38	0.94
	Yes	0.29	0.27–0.30		1.29	1.21–1.37	
Lutein/zeaxanthin	No	0.28	0.27–0.30	0.77	1.30	1.21–1.38	0.89
	Yes	0.28	0.27–0.30		1.29	1.20–1.37	
Smoking status	Never	0.27	0.26–0.29	0.05	1.19	1.10–1.29	0.0003
	Former	0.28	0.27–0.30		1.32	1.24–1.40	
	Current	0.33	0.29–0.37		1.66	1.45–1.87	
Number of eyes with GA	1	0.23	0.21–0.24	<0.0001	0.91	0.81–1.01	<0.0001
	2	0.31	0.30–0.33		1.50	1.43–1.57	
Halo hyperautofluorescence (for eyes with hypoAF at 1st GA; n=184)	No	0.31	0.27–0.35	0.13	1.28	1.07–1.49	<0.0001
	Yes	0.38	0.30–0.45		2.44	2.03–2.85	

All results adjusted for age and sex; 1: results adjusted for square root of GA area at baseline; 2: results adjusted for GA area at baseline; p=p value of interaction between characteristic and year; DD=disc diameters; DA=disc areas; DHA=docosahexaenoic acid; EPA=eicosapentaenoic acid, GA=geographic atrophy

Table 4

Mixed models regression of square root of geographic atrophy area for combined cohort according to genotype.

		Change per year in square root of GA area [1]			Change per year in GA area [2]		
		Estimate (mm)	95% CI (mm)	P	Estimate (mm^2)	95% CI (mm^2)	p
Overall		0.28 (0.16 DD)	0.26–0.30	<0.0001	1.26 (0.54 DA)	1.17–1.34	<0.0001
rs2740488 ABCA1 (0=A, 1=C)	0/0	0.30	0.27–0.32	0.03	1.34	1.22–1.45	0.06
	0/1	0.27	0.24–0.29		1.17	1.04–1.31	
	1/1	0.21	0.14–0.28		0.99	0.62–1.35	
rs2043085 LIPC (0=T, 1=C)	0/0	0.29	0.25–0.34	0.12	1.25	1.01–1.48	0.02
	0/1	0.26	0.24–0.29		1.14	1.01–1.26	
	1/1	0.30	0.27–0.32		1.40	1.27–1.53	
rs2070895 LIPC (0=G, 1=A)	0/0	0.28	0.26–0.30	0.05	1.24	1.14–1.34	0.02
	0/1	0.29	0.26–0.32		1.34	1.19–1.49	
	1/1	0.14	0.01–0.26		0.44	−0.17–1.05	
rs17231506 CETP (0=C, 1=T)	0/0	0.28	0.26–0.30	0.08	1.31	1.19–1.43	0.10
	0/1	0.30	0.27–0.32		1.26	1.13–1.40	
	1/1	0.24	0.19–0.28		1.03	0.81–1.26	
rs5817082 CETP (0=C, 1=A)	0/0	0.27	0.25–0.29	0.52	1.19	1.08–1.30	0.18
	0/1	0.29	0.26–0.32		1.31	1.18–1.45	
	1/1	0.28	0.22–0.34		1.46	1.14–1.78	
rs429358 APOE (0=T, 1=C)	0/0	0.29	0.27–0.31	0.18	1.27	1.17–1.36	0.90
	0/1	0.25	0.22–0.29		1.22	1.05–1.39	
	1/1	0.29	0.09–0.49		1.26	0.25–2.27	
rs73036519 APOE (0=G, 1=C)	0/0	0.25	0.23–0.27	0.001	1.11	1.00–1.23	0.001
	0/1	0.32	0.29–0.34		1.44	1.30–1.57	
	1/1	0.30	0.25–0.35		1.35	1.09–1.61	
rs10490924 ARMS2 (0=G, 1=T)	0/0	0.23	0.20–0.26	<0.0001	1.00	0.86–1.14	<0.0001
	0/1	0.31	0.28–0.33		1.34	1.21–1.46	
	1/1	0.32	0.28–0.35		1.56	1.38–1.75	
rs1061170 CFH (0=T, 1=C)	0/0	0.30	0.26–0.34	0.25	1.52	1.31–1.71	0.01
	0/1	0.27	0.24–0.29		1.16	1.03–1.28	
	1/1	0.29	0.26–0.31		1.25	1.12–1.38	
rs10922109 CFH (0=C, 1=A)	0/0	0.28	0.26–0.30	0.41	1.22	1.12–1.32	0.09
	0/1	0.29	0.26–0.32		1.38	1.22–1.53	
	1/1	0.24	0.16–0.32		0.97	0.55–1.38	
rs61818925 CFH (0=G, 1=T)	0/0	0.28	0.25–0.30	0.15	1.23	1.12–1.35	0.47
	0/1	0.30	0.27–0.32		1.31	1.18–1.44	
	1/1	0.24	0.18–0.29		1.13	0.84–1.42	

		Change per year in square root of GA area [1]			Change per year in GA area [2]		
rs12144939 CFH (0=G, 1=T)	0/0	0.25	0.12–0.39	0.93	0.79	0.11–1.46	0.38
	0/1	0.28	0.23–0.32		1.23	1.01–1.45	
rs800292 CFH (0=G, 1=A)	0/0	0.28	0.26–0.30	0.85	1.24	1.15–1.33	0.55
	0/1	0.28	0.24–0.31		1.30	1.12–1.49	
rs10033900 CFI (0=C, 1=T)	0/0	0.24	0.21–0.27	0.004	1.16	0.99–1.32	0.007
	0/1	0.31	0.28–0.33		1.39	1.27–1.51	
	1/1	0.27	0.23–0.30		1.10	0.94–1.26	
rs17440077 CFI (0=A, 1=G)	0/0	0.27	0.25–0.30	0.70	1.23	1.11–1.36	0.92
	0/1	0.29	0.26–0.31		1.27	1.15–1.39	
	1/1	0.29	0.24–0.33		1.27	1.02–1.52	
rs116503776 C2/CFB (0=G, 1=A)	0/0	0.28	0.26–0.30	0.71	1.26	1.17–1.35	0.91
	0/1	0.30	0.25–0.34		1.25	1.02–1.48	
	1/1	0.26	0.13–0.40		1.10	0.42–1.79	
rs114254831 C2/CFB (0=A, 1=G)	0/0	0.29	0.26–0.31	0.08	1.29	1.17–1.41	0.01
	0/1	0.28	0.26–0.31		1.30	1.17–1.43	
	1/1	0.22	0.17–0.28		0.85	0.57–1.13	
rs2230199 C3 (0=C, 1=G)	0/0	0.31	0.28–0.33	0.0002	1.44	1.33–1.56	<0.0001
	0/1	0.27	0.24–0.29		1.12	0.99–1.26	
	1/1	0.18	0.13–0.24		0.70	0.42–0.98	

All results adjusted for age and sex; 1: results adjusted for square root of GA area at baseline; 2: results adjusted for GA area at baseline; p=p value of interaction between SNP and year; DD=disc diameters; DA=disc areas; GA=geographic atrophy

Table 5A

Multivariate analysis of square root of geographic atrophy area in the combined cohort, with inclusion as covariates those clinical/imaging characteristics that met Bonferroni significance in mixed models regression, together with age and sex.

Effect	Level	Estimate	L95%CL	U95%CL	P	Overall P
Age	_	0.003	0.001	0.01	0.12	0.12
Sex	Male	−0.04	−0.09	0.02	0.17	0.17
	Female	0.00	-	-	-	-
Square root of GA area at baseline, mm	_	1.01	0.96	1.05	<0.0001	<0.0001
GA year	_	0.28	0.27	0.29	<0.0001	<0.0001
Smoking	Former	0.04	−0.01	0.10	0.12	0.03
	Current	0.14	0.03	0.25	0.01	
	Never	0.00	-	-	-	
Education	Some college	−0.08	−0.14	−0.03	0.004	0.01
	Post-graduate	−0.04	−0.11	0.04	0.35	
	HS or less	0.00	-	-	-	
Number of eyes with GA	2	0.14	0.08	0.19	<0.0001	<0.0001
	1	0.00	-	-	-	
Central GA at baseline	Yes	−0.13	−0.19	−0.07	<0.0001	<0.0001
	No	0.00	-	-	-	
GA configuration at baseline	Multifocal	0.13	0.06	0.20	0.0003	<0.0001
	Horseshoe & ring	−0.06	−0.22	0.10	0.45	
	Solid	−0.03	−0.12	0.06	0.57	
	Indeterminate	0.16	0.00	0.31	0.04	
	Small	0.00	-	-	-	

GA=geographic atrophy

Author Manuscript

Table 5B

Multivariate analysis of square root of geographic atrophy area in the combined cohort as per Table 5A, including the interaction term of SNPs and year that met Bonferroni significance in mixed models regression. Each SNP was analyzed separately

SNP	rs73036519 APOE (0=G, 1=C)		rs10490924 ARMS2 (0=G, 1=T)		rs2230199 C3 (0=C, 1=G)	
	Estimate	95% CI	Estimate	95% CI	Estimate	95% CI
0/0	0.25	0.22–0.27	0.23	0.20–0.25	0.30	0.28–0.33
0/1	0.32	0.29–0.34	0.30	0.28–0.33	0.27	0.24–0.29
1/1	0.30	0.25–0.35	0.32	0.28–0.35	0.15	0.09–0.21
p interaction	0.0003		<0.0001		<0.0001	